

Ice Detection of Pure and Saline Ice Using Infrared Signature

¹ Taimur Rashid, Hassan A. Khawaja, K. Edvardsen

Department of Engineering and Safety, Arctic University of Norway (UIT), 9019, Tromsø, Norway

¹ Tel.: +47 98984712

¹ taimur.rashid@uit.no:

Received: Accepted: Published:

Abstract: The paper shows the possible implementation of an Infrared (IR) ice detection technique. In respect of safety in marine operations, saline ice detection can be significant for automated de-icing systems. Experimentation is performed to observe and detect saline and pure ice samples. The discussed detection mechanism is unique and differs from passive IR detection by introducing the self-heating concept. The use of heating information inside the IR ice detection system will enable the improvement of the system's detection capability and the dissemination of valid information at the user interface level. The experimentation shows valid detection of ice and no/ice conditions based on consistent temperature gradients.

Keywords: Icing; infrared; thermal signature; cold region; saline ice.

1. Introduction

In challenging environments, such as below zero temperature conditions, ice accretion can occur at a rapid pace; this can adversely affect marine operations in cold climates. Taking such conditions into account, ice detection can be useful for the mitigation and removal of ice on marine and offshore structures. Various techniques exist in the literature for evaluating ice and snow properties. These techniques utilize the physical and/or electromagnetic properties of ice [1, 2]. The parameters measured by these ice detectors include the mass, rate and liquid water content [3]. Generally, atmospheric icing is detected by most of these detectors. The other type of icing that is a safety concern in marine operations in cold regions is marine icing [4], which is different in nature from atmospheric icing. It involves the influence of sea spray, which is produced from the collision of waves with the ships and wind that shear the high wave crests [5, 6]. The subsequent sea spray

generated by the collision and shearing of waves that travels in the air and freezes on impact with the ship's superstructure or offshore structural elements. If this type of icing continues to occur for a long duration, it can cause an increase in ice loading, which can be hazardous if not mitigated in time. Such icing conditions are also hazardous for human operations. In this case, ice detection can be useful in assisting the anti/de-icing process.

The techniques mentioned above include point and area detection of ice. In marine operations, remote detection of icing can be effective as it can assist in the detection of a larger surface area. Remote monitoring of ice upon surfaces was tested in the aviation industry, where icing on aircraft wings was observed using infrared cameras [7]. The effectiveness for the marine environment of infrared applications in icing needs to be investigated. Apart from the aviation industry, infrared remote monitoring is being used in various industrial applications, where temperature monitoring is critical for larger surface areas. Acquiring a thermal

signature from infrared devices gives the advantage of analysing temperature profiles of the complete system without any direct contact. Studies have shown that infrared cameras can be utilized to monitor cold objects at low temperatures [2, 8-10]. Specific infrared cameras are currently being used in marine operations to detect icebergs floating in the sea; this indicates the possible applicability of infrared devices in the marine environment [11].

This paper aims to show the experimentation setup for the detection of marine icing. The method of detecting pure/saline ice and their water droplets is presented. Lab-setup is explained, taking into account the anti/de-icing techniques used in ships and on offshore structures in the marine environment. Section 2 of the paper explains the major components used for the experimentation; these include an infrared camera, heating elements, surface material, control and monitoring system and icing samples. These setup components are briefly described and can be modified for advanced experimentation. Section 3 explains the experimentation performed to observe the saline and pure icing samples. It also shows the behaviour of water droplets on a heated surface. Section 4 describes the results and presents a discussion regarding thermal gradients in icing/no-icing conditions. The paper concludes in Section 5, summing up the technique's effectiveness regarding ice detection in the marine environment.

2. Setup Components

2.1 Infra-Red (IR) Camera

An IR camera receives an incident IR beam. IR light is electromagnetic radiation that has a longer wavelength, as compared to visible light. It has a spectral range, starting from the edge of the visible red light, from $0.74\mu\text{m}$ to $300\mu\text{m}$. The infrared spectral band is generally sub-divided into four sub-bands: near infrared (NIR) ($0.75\text{--}3\mu\text{m}$), medium wavelength infrared (MWIR) ($3\text{--}6\mu\text{m}$), long wavelength infrared (LWIR) ($6\text{--}15\mu\text{m}$) and very long wavelength infrared (VLWIR) ($15\text{--}1000\mu\text{m}$) [12]. The working principle of an IR camera is based on thermography imaging. The major components of the IR camera are a lens, detector, video processing electronics and user interface control, as shown in Figure 1. The IR camera operates with the incident beam of light focusing on the detector by means of the lens. The detector contains the IR sensitive elements arranged in an array called the focal plane array (FPA). These are IR sensitive elements and miniature in size (micro-meters). The number of elements inside the array determines the resolution of the IR imagery produced by the camera [13]. The processing electronics translate the detector signals into infrared imagery. The processing electronics also control the parameters of the captured imagery. Sets of commands can be given to the processing electronics via the user interface. Currently, the available IR cameras generally include user interface

software to compute the parameters such as scene temperature, calibration, external trigger input and imagery recording. Calibration is often required to read out the correct temperature across the captured scene.

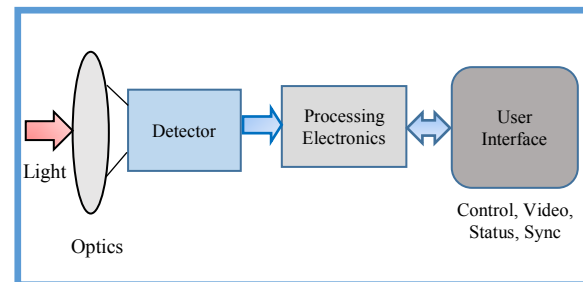


Fig. 1. Components of IR camera

Cold temperature scenes can also be observed with the help of an IR camera. The observation of icing surfaces from IR thermography has been reported in literature [14], but no significant literature is available in respect of marine ice detection in cold regions. Experimentation can be performed to evaluate the capability of IR thermography's application in ice detection for ships and offshore structures.

2.2 Heating Elements

IR thermography for ice detection can be challenging when a uniform scene temperature is observed. The thermographic profile of the cold object and the scene temperature might be the same in some cases, which could lead to false detection of ice. Furthermore, the reflectivity of the ice under certain conditions can indicate a false temperature captured by the IR detectors, which requires calibration. Normally calibration is performed with the known object's temperature, which could be a difficult task to perform repetitively during field operations in a cold, harsh environment. The problem of false detection from IR thermography can be minimized if an active heating mechanism is introduced underneath the platform or the structure upon which ice is accreted. The heating elements will perform a major role in generating the known heat signature when the ice is accreted over it. The heating elements utilized in the experimentation setup could be electro thermal based with strong heat generation capacity. The size of the heating elements should be minimal and compact so that they can be arranged in a flexible manner. A few examples of heating elements that could be tested as an active heating source for the experimentation are Peltier thermoelectric modules (Figure 2a) and thermal resistive elements such as a positive thermal coefficient of resistance (PTC), as shown in Figure 2b.

Peltier thermoelectric modules are solid state devices based on thermoelectric heat pump theory, as they behave like a heat pump and transfer the heat from one side of the device to the other. As the modules withdraw the current, one side becomes immediately hot and the other side becomes cold. The hot temperature can reach up to hundreds of degrees (°C); similarly, the cold side acquires negative temperatures very quickly. On the other hand, positive thermal coefficient of resistance (PTC) heaters work on the principle of resistive heating, where resistance increases upon heating. PTC devices can provide a high-temperature range of up to 150°C or more, depending on the type of resistive material used and the current rating.

These elements discussed are commercially available in miniature sizes (a few centimetres) and can be controlled with DC or AC powered control circuitry. The control mechanism of these heating elements is significant for the experimentation that will be used with an IR user interface capturing mechanism.

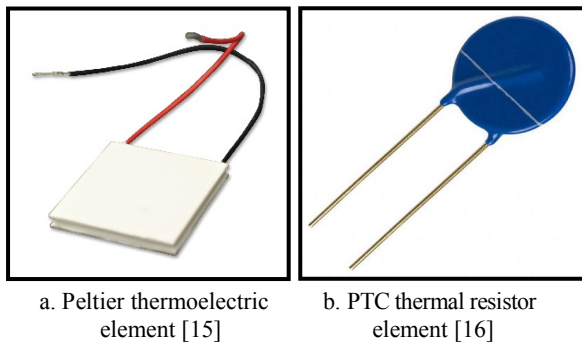


Fig. 2. Heating elements

2.3 Interface

The interface is the overlying material above the heating elements' arrangement. The purpose of the interface is to supply heat through conduction. The heated elements underneath the surface transfer the heat to the icing layer accumulated on the overlying surface. Efficient conducting materials can be used as an interface materials for the experimentation process. Materials with high conductivity, for instance metals such as aluminium, iron, copper etc., can be considered as the interface materials.

2.4 Control Module

The control module consists of electronic circuitry used to control the heating elements. This module recognizes the input from the user interface and drives the heating elements through its digital output lines. The control module executes the image capturing based on producing an external trigger signal. This trigger signal drives the infrared camera to capture the image for that instance. The final imagery is displayed through the imaging interface for temperature profile recording. Thus heated

elements' on/off signals are generated by the control module that is in accordance with the IR imagery profile.

2.5 User Interface

The user interface in this experimentation is the mutual interface of IR imagery analysis software and control module circuitry. The observation of the IR camera software will produce thermal signature and temperature profiles of the icing samples. The control module will generate the operating cycles of the heating elements to produce the imaging profile. The resultant imaging is then analysed to evaluate the captured scene.

2.6 Icing Samples

The pure and marine icing samples were prepared in order to compare their IR signatures. These samples were kept above the heated surface. The pure ice samples were prepared by freezing 10 ml of tap water in a round-shaped container. A similar volume of saline ice samples was prepared by freezing seawater collected from the North Atlantic Ocean. The samples were frozen under similar conditions.

3. Experimental Setup

The experimental setup for marine ice detection comprises of the components discussed in Section 2. An IR camera of MWIR range is used at a normal viewing angle to the icing surface. This was done to avoid any possible reflections that could lead to false temperature detection. The IR resolution of the camera used in the experiment is 320×240 pixels with a temperature sensitivity of 0.05°C. The distance of the IR camera from the icing surface was kept short (60 cm), such that the surface image fits into the camera frame. The reason behind this was to keep the same frame coordinates for analysis and to avoid camera zoom during experimental observations on the user interface. Most of the commercially available IR cameras include a user interface package. The proposed experimentation setup is shown in Figure 3.

Heating control in IR ice detection is provided by the control module, which is responsible for controlling the power on and power off timings of the heated elements. The heating elements discussed can also be used as de-icing agents. Integration of the camera's user interface with the control module helps to synchronize the captured scene with the control mechanism. The infrared energy of a certain temperature is released when the control module drives the heating elements. The selection of individual heated elements provides the flexibility to warm a particular area. This helps the IR energy to be captured at the desired locations. The captured IR signature can be evaluated in the IR user interface software to validate the presence of ice.

The operating mechanism of the experimental setup starts with the capturing of the IR frame without turning on the heating elements. Once the image has been captured, the control module turns on the heating elements and the second IR frame is captured. The images are saved and post processed to evaluate the results. The post processing of the images is performed with the patented software tool that is part of the user interface. The post processing includes the frame calibration, temperature profile extraction and plotting of the results.

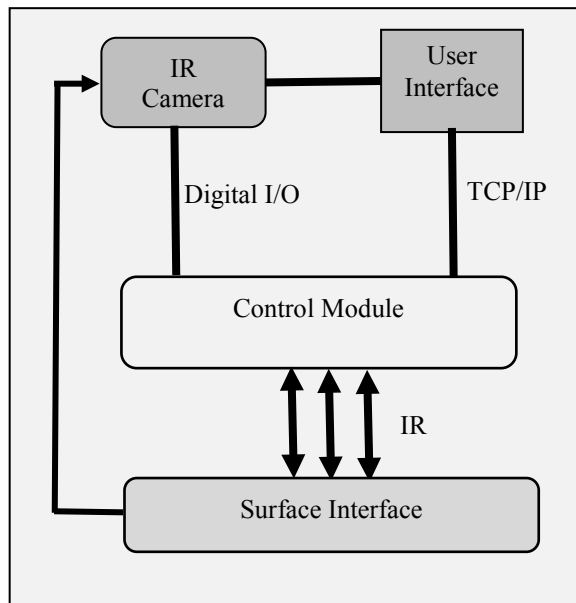


Fig. 3. IR ice detection setup with active heat signature

4. Results and Discussions

The experimentation was performed to observe the infrared signatures of saline and pure ice and water droplets on a heated surface. These experiments were performed at room temperature. The heated elements were operated by the control module. The top of the surface interface was covered with pure ice and saline ice samples, which were prepared in a round-shaped container. The surface area of these samples was 20cm² with approximately 1.2 cm thickness. The ice samples were placed on a heated surface area of approximately 64 cm². The heated elements were operated above 100°C for a short period of time (20-25 seconds). Observations were made of surface temperatures from 23°C to 115°C. The duration to reach the peak temperature was approximately 20 seconds. The IR user interface was used to record infrared signatures of the icing samples. Later, the saline and pure water droplets were observed. The isothermal profiles of these samples are shown from Figure 4 to Figure 7. The temperature profiles across the cross-sectional area of ice samples were observed from the isothermal images (Figure 4 and Figure 5).

At the moment both icing samples were taken out, the minimum surface temperature of the pure icing sample was -4°C and of the saline ice was -15°C. By the time the pure icing sample was placed on the heating surface, the surface temperature had increased to 0.4°C. On the heated surface, the temperature profiles of the pure ice sample showed consistent temperature recordings from 0.4°C to 2°C (Figure 4). The heated surface temperatures during the recordings were 23°C, 80°C, 110°C and 115°C. The presence of pure ice can be asserted with the temperature recordings around 0°C. In the case of non-icing conditions above the surface interface, temperature profiles would have been on the higher scale.

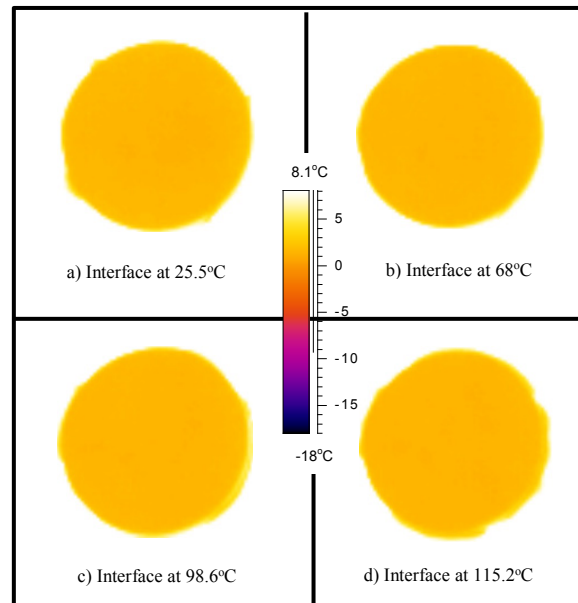


Fig. 4. Pure ice isothermal signature with heating surface

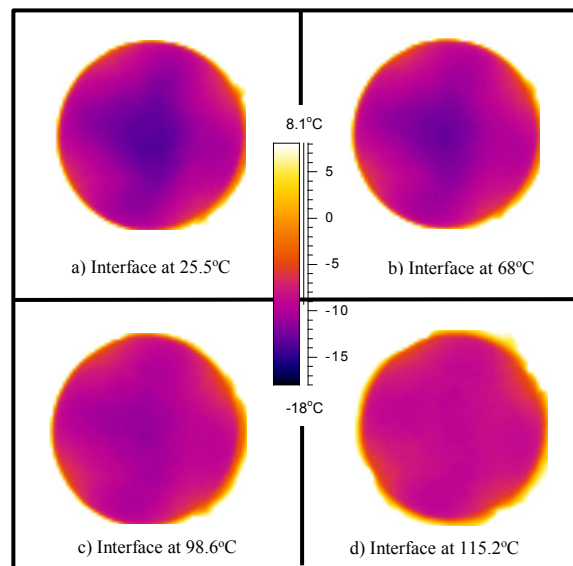


Fig. 5. Saline ice isothermal signature with heating surface

The saline icing sample was much cooler than the pure ice sample during the experimentation process. A very negligible temperature drop was observed as the saline ice sample was taken out of the freezer and placed onto the heated surface. The temperature profiles of the saline ice sample show a steady rise in temperature from -15°C to -5°C (Figure 5) as the temperature of the heated surface increased. The recordings were made on the heated surface at temperatures of 23°C , 80°C , 110°C and 115°C respectively.

The other noticeable results were obtained by observing the pure and saline water droplets of different sizes over the heated surface, as shown in Figure 6 and Figure 7. The isothermal infrared signature shows the presence of droplets in contrast with the rest of the surface.

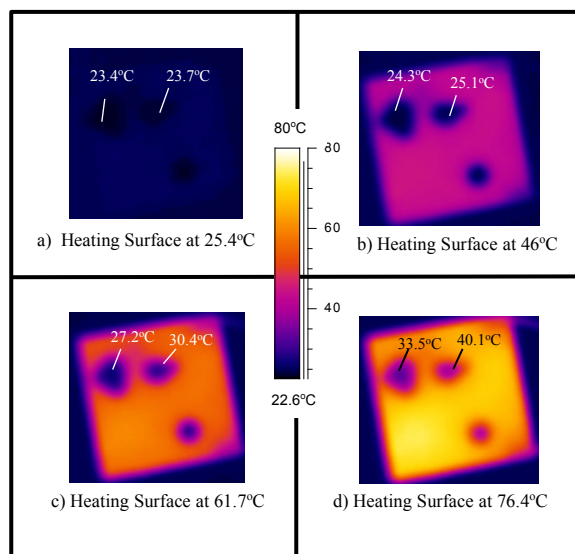


Fig. 6. Pure water droplets isothermal signature on the surface interface

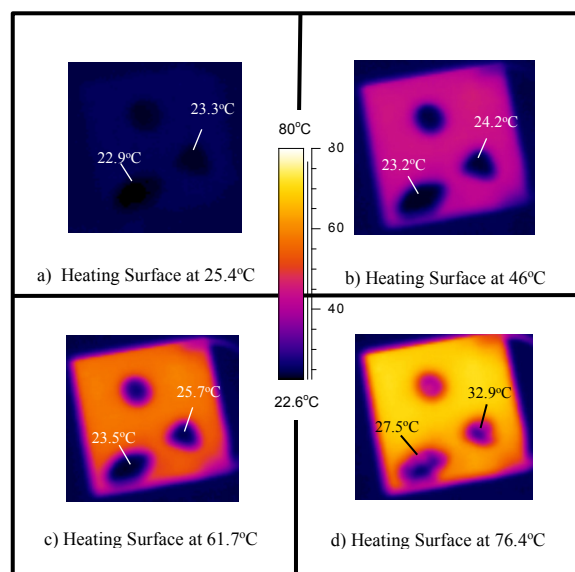


Fig. 7. Saline ice isothermal signature upon heating surface

These observations were recorded at surface interface temperatures of 25.4°C , 46°C , 61°C and 76.4°C . Average temperature recordings of the small and large water droplets were performed (Figure 6).

The water droplets' temperature increased consistently as expected, and a significant difference in the temperature was observed between large and small water droplets (Figure 6). Overall, these droplets could be identified clearly from the rest of the interface.

5. Conclusion

A modified experimentation was performed to test the potential of an IR thermography technique to detect ice. Pure and saline icing samples were observed, along with their respective liquid droplets, on a heated surface. The observations were recorded during rising temperatures from 25°C to 115°C . Observations clearly identify icing and non-icing conditions at room temperature. The water droplets' temperature profiles rise consistently with that of the heated interface. The low conductivity of saline ice, as compared to pure ice, can also be observed from the isothermal images. Overall, the IR signature of icing samples on a heating interface is useful in distinguishing icing and non-icing conditions.

Acknowledgements

The work reported in this paper is funded by the MAROFF, project no. 195153/160, in collaboration with Faroe Petroleum. We would also like to acknowledge the support given by Prof. James Mercer at the University of Tromsø.

References

- [1]. S. Fikke et al., Cost 727: atmospheric icing on structures. Measurements and data collection on icing: State of the Art, *Publication of MeteoSwiss*, 2006. **75**(110): p. 1422-1381.
- [2]. T. Rashid, H. Khawaja, K. Edvardsen, *Determination of Thermal Properties of Fresh Water and Sea Water Ice using Multiphysics Analysis*. *International Journal of Multiphysics*, 2016. **10**(3): p. 277-291.
- [3]. T. Rashid, U. Mughal and M.S. Virk, Feasibility of charge transfer based atmospheric ice detection and measurement, in *International Conference on Sensor Technologies and Applications*, 2014.
- [4]. T. Rashid, H.A. Khawaja, and K. Edvardsen, Review of marine icing and anti-/de-icing systems, *Journal of Marine Engineering & Technology*, 2016: p. 1-9.
- [5]. P. Roebber and P. Mitten, Modelling and measurement of icing in Canadian waters, 1987: *Atmospheric Environment Service*.
- [6]. J. Overland et al., Prediction of vessel icing, *Journal of Climate and Applied Meteorology*, 1986. **25**(12): p. 1793-1806.
- [7]. D. Gregoris, S. Yu, and F. Teti, Multispectral imaging of ice, in *IEEE Canadian Conference on Electrical and Computer Engineering*, vol. 4, 2004.

- [8]. T. Rashid et al., Infrared thermal signature evaluation of a pure and saline ice for marine operations in cold climate, *Sensors & Transducers Journal*, 2015. **194**(11): p. 62-68.
- [9]. T. Rashid, H.A Khawaja and K. Edvardsen, Ice Detection Experimentation Setup Using Infrared and Active Heating, in *International Conference on Sensor Technologies and Applications*, 2016. p. 30-33
- [10]. H. Khawaja, T. Rashid, O. Eiksund, E. Broadal, K. Edvardsen, *Multiphysics Simulation of Infrared Signature of an Ice Cube*. *International Journal of Multiphysics*, 2016. **10**(3): p. 291-302.
- [11]. FLIR®. *Iceberg ahead!* 2016 [cited 2016; Available from: <http://www.flir.eu/marine/display/?id=52805>.
- [12]. B. Stuart, *Infrared spectroscopy*, 2005: *Wiley Online Library*.
- [13]. A. Rogalski, Infrared detectors: an overview, *Infrared Physics & Technology*, 2002. **43**(3): p. 187-210.
- [14]. M. Hori et al., In-situ measured spectral directional emissivity of snow and ice in the 8–14 μm atmospheric window, *Remote Sensing of Environment*, 2006. **100**(4): p. 486-502.
- [15]. Peltier Thermoelectric Module, [cited 2016 20.08.2016], (<http://uk.farnell.com/peltier-elements>).
- [16]. PTC Thermistor, [cited 2016 20.08.2016], (<http://uk.farnell.com/epcos/b59886c0120a070/thermistor-ptc-63v-radial-leaded/dp/2285483>).